

Measurement of electromigration parameters of lead-free SnAg3.5 solder using U-groove lines

Ying-Chao Hsu, De-Chung Chen, P.C. Liu, and Chih Chen^{a)}

National Chiao Tung University, Department of Material Science and Engineering,
Hsin-chu 300, Taiwan, Republic of China

(Received 8 April 2005; accepted 14 July 2005)

Measurement of electromigration parameters in the lead-free solder SnAg3.5 was carried out by utilizing U-groove solder lines and atomic force microscopy in the temperature range of 100–150 °C. The drift velocity was measured, and the threshold current densities of the SnAg3.5 solder were estimated to be 4.4×10^4 A/cm² at 100 °C, 3.3×10^4 A/cm² at 125 °C, and 5.7×10^3 A/cm² at 150 °C. These values represent the maximum current densities that the SnAg3.5 solder can carry without electromigration damage at the three stressing temperatures. The critical products for the SnAg3.5 solder were estimated to be 462 A/cm at 100 °C, 346 A/cm at 125 °C, and 60 A/cm at 150 °C. In addition, the electromigration activation energy was determined to be 0.55 eV in the temperature range of 100–150 °C. These values are very fundamental for current carrying capability and mean-time-to-failure measurement for solder bumps. This technique enables the direct measurement of electromigration parameters of solder materials.

I. INTRODUCTION

Due to increasing environmental concerns, the micro-electronics industry is replacing Pb-containing solders with lead-free solders. In recent publications and reports, SnAg-based solder has emerged as one of the most promising Pb-free candidates to replace the conventional eutectic SnPb solder in flip-chip technology.^{1–3} Moreover, with the increasing miniaturization, the input/output (I/O) pin count of flip chip products has dramatically increased, and bump pitch has decreased rapidly. However, the current that each bump needs to carry continues to increase due to high-performance requirements, further increasing the current density in the solder bumps. Therefore, electromigration (EM) has become an important reliability issue in the Pb-free solder joints.^{3,4}

Several reports have studied the current carrying capability and mean-time-to-failure (MTTF) of lead-free solders.^{5–10} Lin et al. investigated the current-carrying capability of eutectic SnAgCu bumps with 6 μm Ni(P) under bump metallization (UBM), and found that there was no electromigration damage in the bumps after the current stressing by 8.5×10^3 A/cm² at 150 °C for 2338 h.¹⁰ Choi et al. reported that the eutectic SnAgCu bumps with Al/Ni(V)/Cu UBM failed after the current

stressing at 2.25×10^4 A/cm² at 140 °C for 132 h.⁵ Wu et al. conducted a MTTF experiment for SnAg4.0Cu0.5 bumps with thin-film UBM of Al/Ni(V)/Cu and found that the MTTF was 1454 h for the bumps stressed by 5.0×10^3 A/cm² at 153 °C.⁹ However, the important parameters of electromigration near the device operation temperature of 100 °C, such as threshold-current density (J_c), drift velocity, activation energy (E_a), and critical product ($J_c L$) of the lead-free solders are still unknown. In this research, we present a technique to measure the electromigration parameters in Cu/SnAg3.5/Cu ultraviolet (UV) groove line. Atomic force microscopy (AFM) was applied to measure the depletion volume, and thus drift velocity can be calculated. This technique provides a direct measurement of fundamental electromigration parameters for the solders.

II. EXPERIMENTAL

The electromigration parameters of the SnAg3.5 solder were measured using UV groove solder films. This structure allowed us to define the dimension of the solder precisely and to closely observe the microstructural evolution. The fabrication procedure is described as follows: First, a four-inch *p*-type Si wafer was cleaned by a piranha solution (H₂O₂ and H₂SO₄ at the ratio of 1:7) for 10 min at 100 °C. Then, 1200 Å SiO₂ and 1500 Å Si₃N₄ layers were subsequently grown on the wafer by the furnace and plasma-enhanced chemical vapor deposition (PECVD) methods. These two layers served as insulating

^{a)}Address all correspondence to this author.

e-mail: chih@cc.nctu.edu.tw
DOI: 10.1557/JMR.2005.0350

and hard mask layers. The SiO_2 and Si_3N_4 layers were then patterned and etched selectively by reactive ion etching (RIE) to form 50- μm -wide lines on the wafer. Potassium hydroxide (KOH) solution at 60 °C was utilized to etch the unprotected silicon lines for 10 min to form 9.5- μm -deep UV-shaped grooves. Subsequently, metallization layers of Cr, Cu, and Au films with the thickness of 500, 4000, and 500 Å, respectively, were evaporated onto the silicon wafer by an e-beam evaporator. Then the wafer was cut into small pieces of 10 × 10 mm with a UV groove in the middle. For each piece, we electroplated Cu with the current of 0.033 A for 30 min, and then polished away the Cu on the silicon surface. Then another mask was utilized to define a 100- μm opening in the copper line inside the UV groove. The Cu was etched selectively away by an FeCl_3 solution (FeCl_3 :de-ionized water = 1:200). SnAg3.5 solder paste was placed in the UV groove and then reflowed at 250 °C for 1 min. The specimen was then ground and polished. During these procedures, the UV groove protected the solder, and the top Si surface served as a polished stop.

Figures 1(a) and 1(b) illustrate the schematic diagrams of the tilted plan-view and cross-sectional view of the specimen, respectively. The dimension of the solder line was about 9.5 μm in depth, 50 μm in width, and 100 μm in length. The Au film was only 500 Å thick; it was thoroughly consumed and dissolved into the solder during the reflowing process. An intermetallic compound (IMC) of Cu_6Sn_5 formed at the interface of the Cu electrodes and the solder. The samples were then stressed

using various current densities and temperatures, and the direction of the electron flow is indicated by the arrows in Fig. 1(a).

Scanning electron microscopy (SEM) was used to observe the microstructure of the solder stripes, and energy dispersive spectrum (EDS) was used to detect the compositions of the intermetallic compounds. Focused ion beam (FIB) was used to examine the void formation near the interface of the IMC and the solder. Atomic force microscopy (AFM) was used to measure the depletion volume on the cathode side of the samples. The shape of the AFM tip was a pyramid. The tip was 20 nm in diameter, and the tip height was about 15 μm . The mean roughness (R_a) of the solder before electromigration test was 44.03 nm. Contact mode was used in this study, and the maximum height that the AFM can measure is 5.5 μm . To locate the interface of the Cu and the solder, the Si surface near the interface was marked by four laser marks. The estimation of depletion volume was carried out by measuring the volume difference in the range of the four laser marks before and after the current stressing. Due to the polishing process, the solder surface was lower than the silicon surface before current stressing. Therefore, the silicon surface was taken as a reference surface, which was utilized to estimate the depletion volume. Each value was obtained by averaging six scans, and the standard deviation was within $\pm 1.3\%$ compared with the average volume. In addition, the temperature increment due to the Joule heating effect was monitored by an infrared microscope, which has a 0.1 °C temperature resolution and 2 μm spatial resolution.

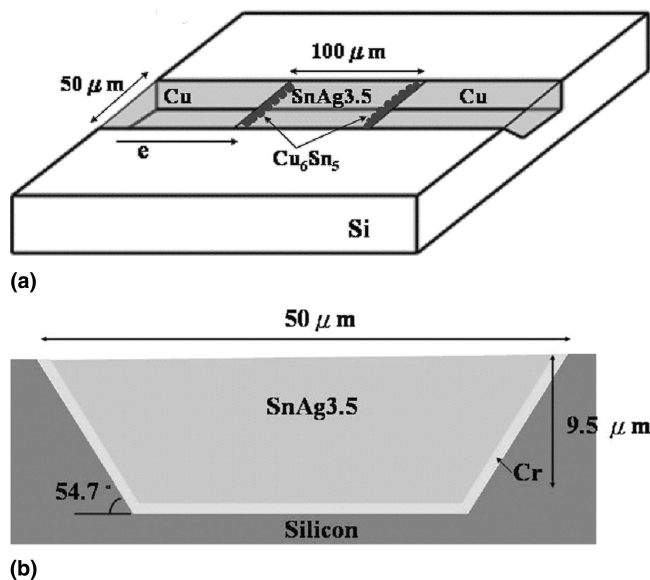


FIG. 1. (a) Tilted plan-view schematic diagram for the SnAg3.5 solder jointed to Cu electrodes in a UV groove line. The direction of the electron flow is indicated by the arrow. (b) Cross-sectional schematic diagram for the UV-groove specimen. Cu_6Sn_5 IMC formed at the bottom and side walls.

III. RESULTS

A. Microstructure of the SnAg3.5 UV groove and temperature measurement

With this technique, solder lines with Cu-solder interface can be fabricated. Figure 2 demonstrates the plan-view backscattered electron (BSE) image of the fabricated UV groove solder line. Cu_6Sn_5 IMC formed at the interface between the electroplated Cu and the SnAg3.5 solder. Cu-Sn IMCs were also observed inside the SnAg3.5 solder matrix, as indicated by the arrows in the figure. The solder line was 105 μm long and 45 μm wide after the lithography and etching. Figure 3 displays the measured temperature increment in the UV groove solder line as a function of applied current density at 100 °C. The highest temperature increment was 15 °C when the specimen was stressed by $1 \times 10^5 \text{ A/cm}^2$. It is evident that the Joule heating effect in the UV groove was much lower than that in a flip-chip solder bump. In flip-chip solder joints surrounded by underfill, the temperature increase due to the current stressing may be easily over 30 °C when $1 \times 10^4 \text{ A/cm}^2$ is applied.¹¹ The reduction

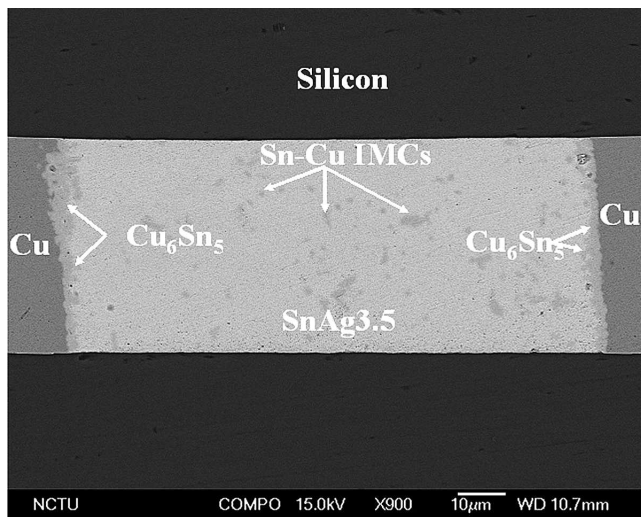


FIG. 2. Plan-view SEM BEI image of the fabricated UV groove specimen.

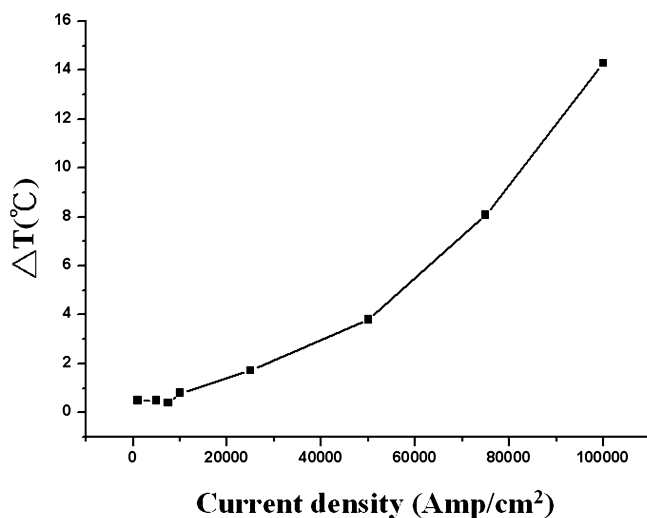


FIG. 3. Measured temperature increment inside the solder line as a function of applied current at 100 °C.

may be attributed to the thin film geometry and the excellent heat conduction of the silicon substrate.

B. Threshold current densities of the SnAg3.5 solder

Drift velocity of electromigration was obtained by measuring the depletion volume after the current stressing. Figures 4(a) and 4(b) show the plan-view BSE images of the Cu/SnAg3.5/Cu solder line in the cathode end before and after the current stressing by 5×10^4 A/cm² at 125 °C for 19 h, respectively. Voids can be seen at the interface between Cu₆Sn₅ intermetallic compounds and SnAg3.5 solder. Figures 4(c) and 4(d) display the corresponding 3D AFM images for the solder lines in Fig. 4(a) and 4(b), respectively. The four laser marks in the Si

surface near the solder line were used to locate the Cu-solder interface at the cathode end. The AFM image in Fig. 4(d) also shows the depletion of solder in the cathode end, which demonstrates that the AFM was capable of measuring the depletion in the solder line. The depletion volume for this specimen was estimated to be 434 μm³ by an in-house computer program. The average drift velocity can be obtained by dividing the depletion volume (ΔV) by the product of the average cross-sectional area and the stressing time. Figure 5 shows the average drift velocity as a function of applied current density at 100, 125, and 150 °C, showing a linear relationship for the three temperatures. The results indicate that the drift velocity increased as the applied current density increased for a given temperature, and it also increased with the increase of the testing temperature at the same stressing current density. To verify whether the solder volume would change due to the thermal effect, another solder line was annealed at 150 °C for 21 h, which was the severest thermal history in this study. The volume change due to the thermal history was about 36.85 μm³, which was within the standard deviation. Therefore, no evident volume change was detected after the thermal treatment.

By extrapolating the fitting line to the zero drift velocity, the threshold-current density (J_c) was obtained. The estimated values are 4.4×10^4 A/cm² at 100 °C, 3.3×10^4 A/cm² at 125 °C, and 5.7×10^3 A/cm² at 150 °C. These values represent the maximum current densities that the SnAg3.5 solder can carry without electromigration damage at the three stressing temperatures. With higher testing temperature, there was lower threshold-current density. To verify if these values are correct or not, three specimens were stressed at current densities below the threshold current densities at the three temperatures. Specimens were stressed at the current density of 4×10^4 A/cm² at 100 °C, 2.8×10^4 A/cm² at 125 °C, and 2.5×10^3 A/cm² at 150 °C for 16 h, and no detectable volume change was found. In addition, the critical product, which is the product of J_c and solder length (L), for the SnAg3.5 solder was calculated, indicating values 462 A/cm at 100 °C, 346 A/cm at 125 °C, and 60 A/cm at 150 °C.

C. Activation energy of SnAg3.5 solder

The average drift velocity due to electromigration is given by Huntigton and Grone¹²

$$v = \frac{J}{C} = BeZ^* \rho j = \left(\frac{D_0}{kT} \right) eZ^* \rho j \exp \left(\frac{-E_a}{kT} \right), \quad (1)$$

where J is the atom flux, C is the density of metal ions, B is the mobility, k is Boltzmann's constant, T is the absolute temperature, eZ^* is the effective charge, ρ is the

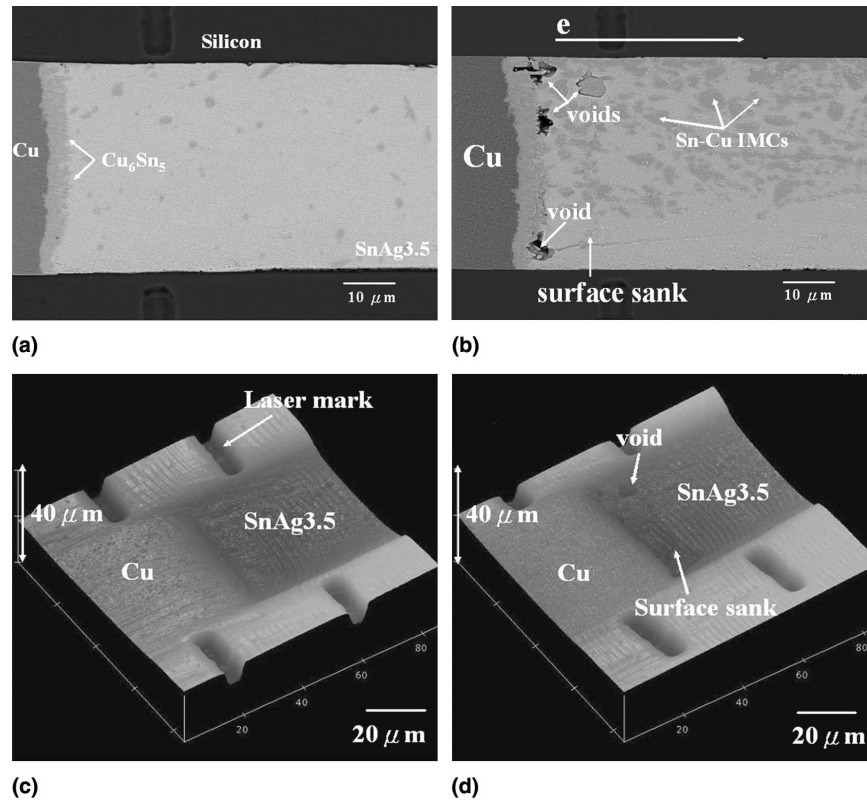


FIG. 4. (a) Plan-view SEM BEI image at the cathode side before current stressing. (b) Plan-view SEM BEI image at the cathode side after the current stressing by $5 \times 10^4 \text{ A/cm}^2$ at 125°C for 19 h. (c) Corresponding AFM image of (a). (d) Corresponding AFM image of (b). SnAg3.5 solder near the interface was partially depleted by the applied current.

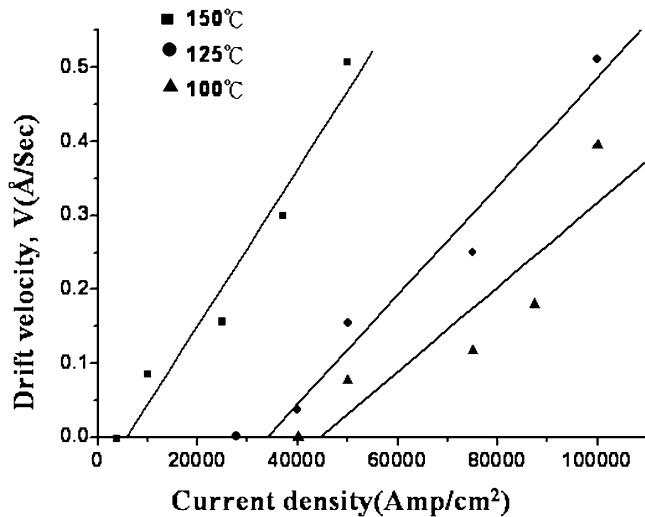


FIG. 5. Average drift velocity of the SnAg3.5 solder as a function of applied current density. The threshold current densities were obtained by extrapolating the fitted lines to zero drift velocity.

metal resistivity, j is the electrical current density, E_a is the activation energy of diffusion, and D_0 is the prefactor of diffusion constant. Equation (1) can be rewritten as

$$\frac{vT}{j} = \frac{D_0 e Z^* \rho}{k} \exp\left(\frac{-E_a}{kT}\right) \quad (2)$$

Taking logarithm of the both sides of Eq (2)

$$\ln \frac{vT}{j} = -\left(\frac{E_a}{kT}\right) + \ln \frac{D_0 e Z^* \rho}{k} \quad (3)$$

Therefore, by measuring drift velocity as a function of reciprocal temperature, the activation energy (E_a) can be obtained. Figure 6 shows the plot of $\ln(vT/j)$ as a function of the reciprocal temperature. The activation energy (E_a) can be determined from the slope of the fitted line, and its value is 0.54 eV in the temperature range of 100–150 °C. However, the temperature in the solder needs to be calibrated due to Joule heating effect, as shown in Fig. 3. The real temperatures in the solder during the current stressing were higher than the ambient ones. The activation energy was calculated to be 0.55 eV using the corrected temperatures.

IV. DISCUSSION

In our samples, the cross-sectional area of the solder at the cathode side gradually decreased during the current stressing. This decrease consequently increased the current density in the solder line, which caused the inaccuracy in estimating the current density. The largest depletion of solder in this research was controlled within $1.5 \mu\text{m}$ in depth. Thus, the current density increment was

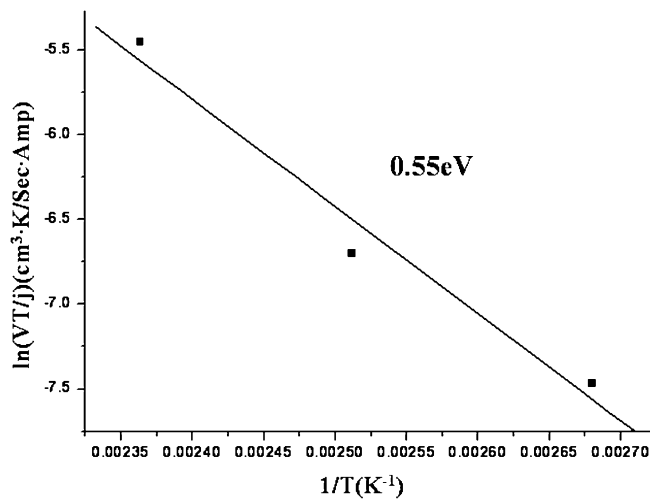
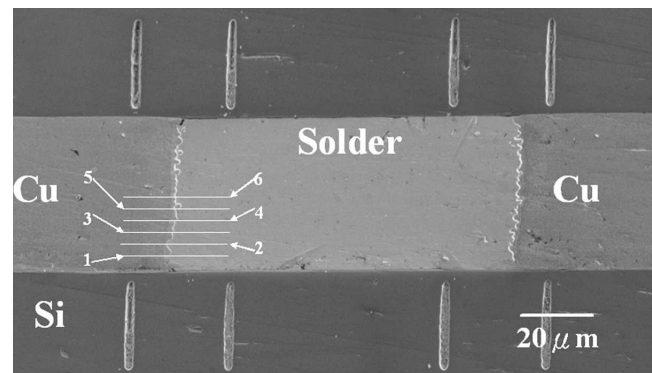


FIG. 6. Plot of the $\ln(vT/j)$ as a function of reciprocal temperature. The activation energy of 0.55 eV was obtained from the slope of the fitted line.

controlled within 22% for the testing samples. Through theoretical calculation, around 86% of the applied current drifted in the solder line, 13% in the IMC layer, and only 1% in the Cr layer. However, from our plan-view SEM images in Figs. 2 and 3, and cross-sectional FIB images in Figs. 7 and 8, no IMC was found on the bottom and side walls of the UV groove. Therefore, the IMC was assumed to spall into the solder completely. Consequently, we assumed that all the current flowing through the solder line. A major advantage of this technique is that there is little current crowding effect in the interface of the Cu and the solder, so the current density can be estimated precisely.

To examine whether the measured threshold current densities are reasonable, we compare the results to other published data. Wu et al. conducted an MTTF experiment for SnAg4.0Cu0.5 bumps with thin-film Al/Ni(V)/Cu UBM), and found that the MTTF was 1454 h for the bumps stressed by 5.0×10^3 A/cm² at 153 °C.⁹ In contrast, the measured threshold-current density was 5.46×10^3 A/cm² at 150 °C in our Cu/SnAg3.5/Cu UV groove sample. Although the solder they used was different from ours, the composition and the melting point of our solder should be quite close, since the composition of the SnAg3.5 solder may approach SnAg4.5Cu0.5 after being reflowed into the UV groove with two Cu electrodes. We speculated that the above discrepancy is due to the serious current crowding effect in the line-to-bump configuration in the flip chip solder joints. From our previous study, the maximum current density near the solder close to the entrance point of Al trace was much higher than the average value in the solder itself.^{11,13} In addition, our previous simulation study showed that the current crowding ratio may be as high as 23 inside the solder for the joints with thin film Ni(V)/Cu UBM, which



(a)



(b)

FIG. 7. (a) Plan-view FIB image of an UV groove before ion etching. (b) Tilted-view FIB image of the UV-groove on the cathode end after ion etching. A void was found in the interface of the IMC and the solder.

means that the maximum current density near the solder close to the entrance point of Al trace is 23 times higher than the average value.¹⁴ Therefore, the real current density in the solder near the Al entrance should be much larger than 5×10^3 A/cm² for the flip chip samples. In our UV groove structure, there will be current crowding effect merely due to the line-to-line structure. In addition, the Joule heating effect would be more serious in the flip chip solder joints than that in the UV groove sample. On the other hand, Lin et al. applied 8.5×10^3 A/cm² at 150 °C in SnAgCu bumps with the 6 μm Ni(P) UBM, and they found no obvious damage after 2338 h stressing. The current crowding effect was relieved greatly by the thick UBM.¹⁴ Therefore, the threshold-current density at 150 °C might be less than 8.5×10^3 A/cm². Based on the above discussion, our estimated threshold-current density seems to be reasonable.

During electromigration test, voids may be generated inside the solder line, and they could not be detected by the surface scanning of AFM. To examine whether there are hidden voids that formed inside the solder line during electromigration, FIB was used to examine the IMC/solder interface on the cathode end. Figure 7(a) show the

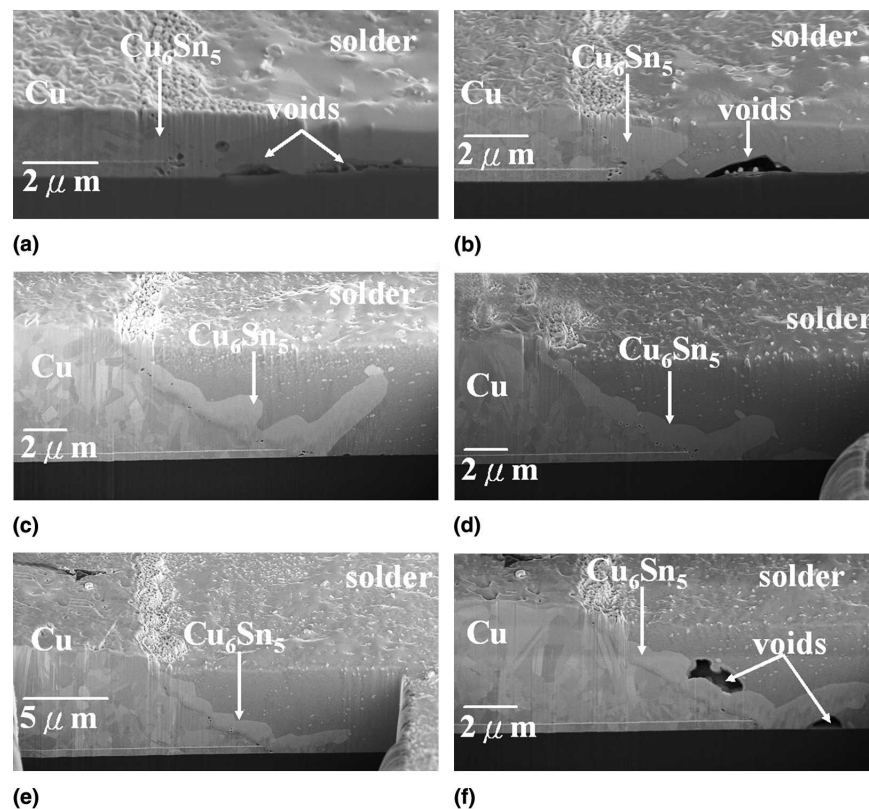


FIG. 8. Tilted FIB images for the cathode end of the UV-groove: (a) cross section 1, (b) cross section 2, (c) cross section 3, (d) cross section 4, (e) cross section 5, (f) cross section 6 in Fig. 7(a). The spacing between adjacent cross sections was about 5 μm .

FIB image of the UV-groove sample before ion etching. The sample was stressed under the current density of $9 \times 10^4 \text{ A/cm}^2$ at 100°C for 10 h. The depletion volume on the cathode end measured by the AFM was $206 \mu\text{m}^3$. Figure 7(b) shows the tilted FIB image for the sample in Fig. 7(a) after ion etching on the cathode end. The sample was etched laterally near the interface of the IMC and the solder, and approximately half of the interface was examined. Six FIB images were taken during the etching process, and their positions were marked by the six white lines in Fig. 7(a). Figures 8(a) to 8(f) show the tilted FIB images for the six cross-sections. Some hidden voids were found inside the solder. However, some of the voids away from the interface might be generated during re-flowing process, not due to electromigration. For example, the void in Fig. 8(b) might be due to the poor adhesion of the solder and the UBM. Nevertheless, the larger void near the interface in Fig. 8(f) may form due to electromigration, and it cannot be detected by the AFM scanning. As a rough estimation, the volume of the hidden voids may be about 10–20% of the depletion volume measured by AFM. It indicates that the depletion volume measured by AFM may be the lower bound of the total depletion volume. Therefore, the real threshold current densities may be slightly lower than the estimated values in this study.

V. CONCLUSIONS

We have successfully developed a technique to measure the parameters of electromigration in lead-free SnAg3.5 solder by using Cu/SnAg3.5/Cu UV groove solder lines at a temperature range from 100 to 150°C . Our results indicate that the threshold current densities were $4.4 \times 10^4 \text{ A/cm}^2$ at 100°C , $3.3 \times 10^4 \text{ A/cm}^2$ at 125°C , and $5.7 \times 10^3 \text{ A/cm}^2$ at 150°C . The critical products of SnAg3.5 solder were calculated to be 462 A/cm at 100°C , 346 A/cm at 125°C , and 60 A/cm at 150°C . The activation energy of SnAg3.5 solder was measured to be 0.55 eV .

ACKNOWLEDGMENT

The authors would like to acknowledge the financial support from the National Science Council of Taiwan through Grant No. NSC92-2216-E009-008.

REFERENCES

1. K.N. Tu, A.M. Gusak, and M. Li: Physics and materials challenges for lead-free solders. *J. Appl. Phys.* **93**, 1335 (2003).
2. D. Suraski and K. Seelig: The current status of lead-free solder alloys. *IEEE Trans. Electron. Pack. Mfg.* **24**, 244 (2001).
3. K. Zeng and K.N. Tu: Six cases of reliability issues of Pb-free

- solder joints in electronic packaging technology. *Mater. Sci. Eng. Rep.* **R38**, 55 (2002).
4. K.N. Tu: Recent advances on electromigration in very-large-scale-integration of interconnects. *J. Appl. Phys.* **94**, 5451 (2003).
 5. W.J. Choi, E.C.C. Yeh, and K.N. Tu: Mean-time-to-failure study of flip chip solder joints on Cu/Ni(V)/Al thin-film under-bump-metallization. *J. Appl. Phys.* **94**, 5665 (2003).
 6. T.Y. Lee, K.N. Tu, and D.R. Frear: Electromigration of eutectic SnPb and SnAg3.8Cu0.7 flip chip solder bumps and under-bump metallization. *J. Appl. Phys.* **90**, 4502 (2001).
 7. S.Y. Jang, J. Wolf, W.S. Kwon, and K.W. Paik: UBM (under bump metallization) study for Pb-free electroplating bumping: Interface reaction and electromigration, in *Proceedings of the 52nd Electronic Components and Technology Conference, San Diego, CA* (IEEE Components, Packaging, and Manufacturing Technology Society, IEEE, New York, 2002), p. 1213.
 8. Y.C. Hsu, T.L. Shao, C.J. Yang, and C. Chen: Electromigration study in SnAg3.8Cu0.7 solder joints on Ti/Cr–Cu/Cu under-bump metallization. *J. Electron. Mater.* **32**, 1222 (2003).
 9. J.D. Wu, C.W. Lee, P.J. Zheng, C.B.J. Lee, and S. Li: Electromigration reliability of SnAg₃Cu_{0.7} flip chip interconnects, in *Proceedings of the 54th Electronic Components and Technology Conference, Las Vegas, NV*, (IEEE Components, Packaging, and Manufacturing Technology Society, IEEE, New York, 2004), p. 961.
 10. J.K. Lin, J.W. Jang, and J. White: Characterization of solder joint electromigration for flip chip technology, in *Proceedings of the 54th Electronic Components and Technology Conference, New Orleans, LA*, (IEEE Components, Packaging, and Manufacturing Technology Society, IEEE, New York, 2003), p. 816.
 11. T.L. Shao, S.H. Chiu, C. Chen, D.J. Yao, and C.Y. Hsu: Thermal gradient in solder joints under electrical current stressing. *J. Electron. Mater.* **33**, 1350 (2004).
 12. H.B. Huntington and A.R. Grone: Current-induced marker motion in gold wires. *J. Phys. Chem. Solids* **20**, 76 (1961).
 13. T.L. Shao, Y.H. Chen, S.H. Chiu, and C. Chen: Electromigration failure mechanisms for SnAg3.5 solder bumps on Ti/Cr–Cu/Cu and Ni(P)/Au metallization pads. *J. Appl. Phys.* **96**, 4518 (2004).
 14. T.L. Shao, S.W. Liang, T.C. Lin, and C. Chen: Three dimensional simulation on current density distribution in flip-chip solder joints under electrical current stressing. *J. Appl. Phys.* **98**, 044509 (2005).